Research Article

Eddy Correlation Measurements of Ozone Fluxes over Coastal Waters West of Ireland

Philip McVeigh, Colin O'Dowd, and Harald Berresheim

School of Physics, Centre for Climate and Air Pollution Studies, National University of Ireland, Galway, Ireland

Correspondence should be addressed to Harald Berresheim, harald.berresheim@nuigalway.ie

Measurements of ozone fluxes using the eddy-correlation (EC) technique were carried out for the first time at the Mace Head atmospheric research station, on the west coast of Ireland between August-October 2009. Vertical exchange of ozone was measured from a tower platform at 22 m above mean sea level to study fluxes over coastal waters excluding the tidal region. The results were averaged over 30 min and exhibited predominantly downward but also upward transport of ozone in the boundary layer. Data quality was found to be high based on inspection of cospectra and micrometeorological measurements. During the study period, a major physical influence on O_3 fluxes was found to be wind speed. Measured fluxes were of the same magnitude as reported in previous open ocean studies ranging from approximately $+0.2$ to $-0.5\,\mu g\,m^{-2}\,s^{-1}$ ($-0.017\,\mu g\,m^{-2}\,s^{-1}$ on average, corresponding to a deposition velocity of $0.25\,mm\,s^{-1}$ or a surface resistance of $4.13\,s\,mm^{-1}$). These results are considered to represent ozone fluxes over shallow coastal waters west of Ireland for conditions during summer and fall not affected by phytoplankton blooms.

1. Introduction

Tropospheric ozone has potential negative impacts on human health and vegetation, and also acts as an important greenhouse gas. Background ozone levels at Mace Head Research Station in western Ireland, currently at an annual average of 35 ppbv, have shown a steady increase over the past two decades at an overall rate of 0.31 ppbv/year between 1987 and 2007 [1]. During the same period the relative contribution to these increasing ozone levels from air advected over the North Atlantic has also significantly grown. Deposition of ozone to surface ocean waters via physical uptake (solubility, turbulent mixing) and chemical reactions in the surface layer [2–4] likely constitute a significant, albeit highly variable "buffer" curtailing the rate of ozone increase in this region.

It has been proposed that ozone can be rapidly degraded by chemical reactions with biogenically produced compounds such as iodide in surface seawater [5–7] leading to the release of iodine compounds followed by rapid particle nucleation [8]. Recent measurements over the northern coast of France by Whitehead et al. [9] appear to confirm the link

between ozone deposition fluxes to exposed tidal flats and the reactions of ozone with volatilized iodine compounds producing new particles and contributing to particle growth and formation of cloud condensation nuclei. This study was primarily aimed at understanding particle production involving ozone deposition over tidal regions whereas very little is known to date about the potential importance of this process over open ocean waters.

The spatial extent of tidal regions is insignificant compared to the open ocean water scale. It has been shown that despite its moderate water solubility the physical removal of ozone by air-sea exchange can be substantial at high wind speeds, increasing by a factor of up to five as wind speed increases from 0 to $20\,m\,s^{-1}$ [6]. Nevertheless, ozone deposition velocities over ocean waters are relatively low compared to exposed tidal or continental regions (typically $<0.1\,cm\,s^{-1}$) and are therefore difficult to measure. Due to these challenging conditions, very few corresponding field measurements have been conducted up to now [9–12].

Future model simulations and predictions of ozone removal rates in North Atlantic marine air are in progress to establish a baseline for the seasonal ozone influx to western

Europe and, specifically, to Ireland (see [13] this issue). The biochemical removal rate of ozone may also exhibit a seasonal signal in conjunction with phytoplankton blooms occurring mainly during spring and summer. Therefore, model improvement requires complementary direct measurements of ozone deposition fluxes to surface seawater over at least one full seasonal cycle. In the present paper we report first data for ozone fluxes measured by eddy correlation at the Mace Head Atmospheric Research station during the period August–October 2009. The primary goal of this study was to provide a data base for large-scale model simulations by measuring ozone fluxes over continental shelf waters excluding tidal regions.

2. Experimental

The Mace Head observatory is located on the west coast of Ireland ($53°20'$N, $9°54'$W). The local meteorology, research facilities, and measurement programme have previously been described in detail by Jennings et al. [14] and O'Connor et al. [15]. Mace Head is located on a peninsula with the oceanic footprint from the North Atlantic corresponding to the local $220°$–$320°$ wind sector. On a yearly average, westerly winds from this sector prevail (55%), the average wind speed is $7 \, \text{m s}^{-1}$, and water depths within the flux footprint vary between 10–33 m.

In August 2009, a Rapid Ozone Flux Instrument (ROFI; [16]) based on the technique developed by Gusten et al. [17], was installed on top of the 22 m tower at Mace Head. The shoreline in front of the 22 m tower is inhomogeneous, rocky, and slanted with a tidal region that extends from 80 m to 180 m away from the base of the tower. The tower is supported by guy wires to reduce vibrations, and has been constructed in order to minimize shadowing on sensors or obstruction to airflow from the marine sector.

Previous footprint and micrometeorological analyses by Norton et al. [18] and Kunz and de Leeuw [19] under marine air mass conditions had shown that flux measurements from the top of the tower (22 m) maximize the oceanic footprint. This has also been confirmed by further micrometeorological studies at Mace Head which established relationships between wind speed and CO_2 flux [20] and between wind speed and primary marine aerosol fluxes [21, 22].

In addition to the ROFI instrument, the eddy flux system used in the present study included a three-dimensional ultrasonic anemometer (Sonic R3; Gill) measuring the three orthogonal wind velocity components u, v, w at 10 Hz, a UV photometric ozone analyser (model 49i; Thermo Scientific) measuring ambient O_3 mixing ratios at 22 m height with a 1 min resolution, and an open path, nondispersive H_2O/CO_2 infrared gas analyser (LI-7500; Licor). The latter instrument was used to obtain water vapour data for the Webb correction (see next section), and the CO_2 data were used to identify and remove rainfall periods from the O_3 flux records.

The ROFI recorded ozone fluctuations at 10 Hz by measuring the chemiluminescence generated from the reaction of O_3 with a coumarin-based dye coated on a disc installed perpendicular to the sample air stream across from a photomultiplier tube. The temperature of the disc was maintained at $30°$C, and the sample flow rate was kept at 100 litres per minute according to the users manual. The intake tubing length and diameter were 5 m and 0.019 m, respectively. The raw voltage signals from the ROFI were calibrated in ppbv units based on the 1 min resolution measurements of the UV photometric analyzer. The effective coating on one disc lasted on average for about 3–5 days after which a new disc was prepared and installed.

The system components were located on the marine sector side of the tower. The anemometer head, the Licor head, and the ROFI intake tubing were all colocated on the end of a 3 m boom extending towards the marine sector, with minimal separation between the ROFI intake and the sonic head (0.1 m in the vertical, 0 m in the horizontal plane). The boom was supported by an extended arm to reduce vibrations in the vertical and horizontal planes, and the anemometer head was leveled with the horizon to decrease errors in subsequent coordinate rotations.

3. Theory

Eddy covariance (EC) is a direct micrometeorological technique for measuring turbulent fluxes in the atmospheric boundary layer. The peak of the spectrum of eddy size depends on the measurement height, the surface roughness height, and wind speed, since eddies increase in size with height and decreased surface roughness. A scalar flux can be measured provided the instrumentation is sufficiently fast-response (10–20 Hz) to capture the dominant range of eddy sizes contributing to the flux.

In general, it is assumed that EC measurements made at one point are representative of the area upwind and that the footprint is large enough for the entire fetch to fall within it. It is also assumed that most net vertical transfer is carried out by eddies, and that there are no low-frequency trends in the data (*stationarity requirement*). Application of a 5 min running mean (high-pass filter) ensured that the stationarity requirement was met, and data were subsequently checked to verify that the running mean was correctly applied. Such detrending may cause a slight underestimation of flux but can be compensated for through spectral analysis [23]. However, such corrections were not applied since corresponding changes in absolute flux magnitudes amount to less than 18% having no effect on flux direction [20].

The height-independent bulk transfer process for heat or trace gases is treated as the sum of the turbulent transfer of the scalar variable from a height z (m) above the surface in question, to the zero plane displacement height, d (m) as well as the transfer across a diffusive sublayer that extends a few millimetres above the surface. Both of these pathways can be represented by resistances, assuming that no storage or chemical conversion occurs within the measurement height on the scale of turbulent transport [24].

The aerodynamic atmospheric resistance (r_a) is used to represent the first pathway, and is calculated assuming gradient transport theory. This resistance depends on turbulent intensity, which in turn depends on atmospheric stability. An additional resistance representing the near-surface laminar

sublayer (r_b), across which transport is governed by molecular diffusion to the surface, represents the second pathway, and can vary spatially and temporally, providing the main resistance to deposition. The total resistance r_t is defined as

$$r_t = r_a + r_b + \cdots = -\frac{X_{O_3}}{F_{O_3}} = -\frac{1}{v_d}, \tag{1}$$

where v_d represents the deposition velocity, and X_{O_3} and F_{O_3} represent the ozone concentration and ozone flux at the measurement height, respectively. The aerodynamic and molecular sublayer transport define the maximum possible deposition velocity. Additional resistance terms due to other processes may be inferred from the difference between total flux measurements and the computed resistance terms.

4. Data Reduction

As already described in Section 2, rainfall contaminated data periods were removed as well as periods with wind directions outside of the marine sampling sector. To ensure that data quality from the ROFI was satisfactory, a procedure was implemented to identify and discard erroneous or low-quality data points. The first few hours of a disc sampling period sometimes contained spurious values, and so all data up to 2 hours immediately after renewing a disc were removed. Ozone mixing ratios obtained from the UV photometric instrument were plotted against ROFI output voltages for each sample disc at a 1 min resolution as well as the ratios between both data sets. Outliers and periods of questionable data were removed, especially towards the end of a disc sampling period, when sensitivity was reduced to about 1-2 V output signal. A more detailed description of this procedure can be found in Muller et al. [25]. In order to maximize correlation, corresponding data sets were phase-shifted to compensate for any time delays in the data logging process. The time delay for the ROFI instrument was calculated to be 0.85 sec based on intake tube dimensions and flow rate (see Section 2).

Ultrasonic anemometer temperature data were used to calculate the virtual air temperature, which was then corrected for water vapour fluctuations to obtain the true air temperature. Performing a running mean on data sets acted like a recursive high-pass filter, whereby lower frequency trends were attenuated by using a running mean time constant of 5 min. Coordinate rotations were applied in order to minimize errors caused by vertical advection or human error in sonic leveling. Two-dimensional coordinate rotations were used, and basically pointed $\overline{u}$ in the direction of mean incident air flow by minimizing $\overline{v}$ and $\overline{w}$ to zero.

Covariances were calculated and then block-averaged over 30 min periods to yield momentum flux (τ), friction velocity (u^*), drag coefficient (C_D), roughness length (z_0), sensible heat flux (H), latent heat flux (LE), and Monin-Obukhov length (L). The latter was used to define a dimensionless scaling parameter, z/L, to define the thermal stability state of the boundary layer.

Three different methods were applied to obtain ozone fluxes: the Ratio Method (RM), the Ratio Offset Method (ROM), and the Disc calibration method (DCM). For the RM method, raw covariances of the vertical wind component with the raw O_3 signal (voltages from the ROFI), were divided by the mean voltage to provide the deposition velocity, which was then multiplied by the absolute ozone concentration. This method assumes that the voltages are proportional to the absolute concentrations including a zero offset. The ROM method is based on the RM method, with a modification that accounts for the offset (mean output at zero ozone concentration) in the analyser. The offset was obtained by calculating the intercept of ozone concentrations plotted against voltages by using 1 min averages for each hour of data. The DCM method applies a calibration factor to the raw flux for each disc period, which was obtained by calculating the slope of the relationship between the output voltage and O_3 concentration. This calibration factor was then multiplied by the raw flux to obtain absolute ozone fluxes. A detailed comparison of these three methods can be found in Muller et al. [25].

In a further step, the Webb correction [26] was applied to the fluxes of H_2O and O_3. A small but significant vertical velocity known as the Webb velocity may arise from the fact that turbulent motion can also consist of ascending or descending air parcels due to density differences and must be taken into account when evaluating EC flux measurements.

The water vapour flux was corrected for density variations due to temperature fluctuations which was then used along with the temperature flux to calculate the Webb velocity:

$$\overline{w} = \mu \frac{\overline{w'q'}}{\rho_d} + (1 + \mu\sigma)\frac{\overline{w'T'}}{\overline{T}}. \tag{2}$$

Here, μ is the ratio of the molecular masses of air to water (1.6077), σ is the ratio of moist and dry air densities, and ρ_d is the density of dry air. The resulting Webb velocity was then applied to the raw O_3 flux:

$$F_{X,O_3} = \overline{w'X'_{O_3}} + \overline{w}\overline{X_{O_3}}. \tag{3}$$

The filtering of data was divided into two main categories, and only data meeting certain criteria were retained.

(1) Filtering for an *oceanic footprint*.

   (a) *Wind direction* ($220° \leq WD \leq 320°$). Data with a wind direction outside this range were removed to obtain an oceanic fetch.

   (b) *Stability* ($-2 \leq z/L \leq 2$). Data with a stability scaling parameter outside this range were removed to ensure that extreme stability cases were excluded. This was also the range investigated by Kaimal et al. [27], making cospectral comparisons more relevant.

   (c) *Source Region* ($\geq 90\%$ of cumulative normalized contribution to flux, CNF, at ≥ 700 m distance from tower). Data points that had more than 10% of their CNF within 700 m distance of the tower were removed to exclude any remaining influences from exposed land surfaces.

(2) Filtering for *data quality.*

    (a) *Wind speed variability* ($\sigma_{U_{22}} \leq (U_{22}/7.5)$). Data points with a high 22 m level wind speed variability (or standard deviation, $\sigma_{U_{22}}$) were removed assuming $U_{22}/7.5$ as a suitable cutoff level.

    (b) *Correlation between raw O_3 signal voltages and O_3 concentrations.* If the correlation coefficient between these two variables was <0.5 for any 30 minute period, the data was deemed unsatisfactory. Correlation coefficients were computed using the same data used for computing the offsets and calibration factors for the ROM and DCM methods.

5. Results and Discussion

Figure 1 shows the results of the filtered data set consisting of 69 half-hour periods. The three methods used to determine ozone fluxes (RM, ROM and DCM) produced nearly identical results. Therefore, only fluxes obtained using the ROM method are presented. O_3 fluxes ranged from +0.2 to $-0.5 \, \mu g \, m^{-2} \, s^{-1}$ ($-0.017 \, \mu g \, m^{-2} \, s^{-1}$ on average, corresponding to a deposition velocity of $0.25 \, mm \, s^{-1}$ or a surface resistance of $4.13 \, s \, mm^{-1}$). The large variability and range of fluxes observed here are comparable to values reported previously for other coastal areas [9, 11, 12] as well as recent shipboard measurements over open ocean regions [10]. Daytime and nighttime periods are also indicated in Figure 1. Corresponding average fluxes were $-0.038 \, \mu g \, m^{-2} \, s^{-1}$ and $-0.021 \, \mu g \, m^{-2} \, s^{-1}$, respectively, which suggest a diurnal cycle similar to what has been reported by Gallagher et al. [11]. However, the difference between both values was not statistically significant.

Data loss resulted mostly from data filtering due to out-of-sector wind conditions, rainfall, and poor disc quality. Four distinct periods can be identified from Figure 1. O_3 fluxes during the third period (early October, yearday 276–278) were conspicuously low and virtually zero. The data were deemed to be sound since no evidence was found for malfunction of the instruments during the corresponding period. Therefore, cospectra of all O_3 fluxes with values between $|0.01|$ and $|0.02| \, \mu g \, m^{-2} \, s^{-1}$ were averaged and are shown as a single line (wX) in Figure 2, approximating to the temperature cospectra (wT). Since smaller high-frequency eddies transport scalars more effectively than lower frequency eddies, they are of most interest here. The theoretical ideal slope described by Kaimal et al. [27] displaying a $-4/3$ power law is shown for comparison. It agrees well with both the wX and wT cospectra at higher frequencies. This shows that the data were of good quality and suggests that noise was negligible in this frequency range.

Back trajectories of air masses were evaluated for each measurement period. Figure 3 shows an example for September 6 (yearday 250) which, overall, was typical for the periods shown in Figure 1. Therefore, the variations found in the data were likely not caused by major changes in air mass composition. As outlined in Section 2, any influence by
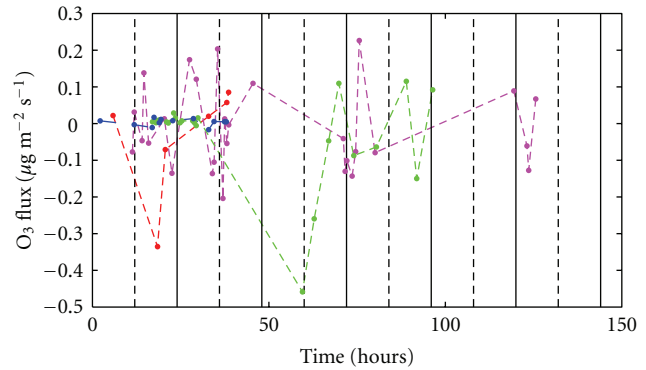

FIGURE 1: Time series of 30 min averaged O_3 fluxes (dots) during August–October 2009 showing the four main measurement periods; red: 28-29 August (Yearday 240-241), magenta: 4–9 September (Yearday 247–252), blue: 3-4 October (Yearday 276–278), and green: 22–26 October (Yearday 295-299). Time in hours from 00:00 on the first day of each period is shown on the x-axis, with 12:00 and 00:00 marked sequentially with a dotted and solid vertical line, respectively.

tidal movements on the recorded fluxes was expected to be negligible (see also Figure 5). Footprint contributions were calculated and averaged for 30 min periods based on the model by Schuepp et al. [28]. The model applies to neutral stability conditions which were predominant during all study periods and typically prevail at Mace Head during westerly flow due to moderate to high wind speeds producing a well-mixed boundary layer [22]. A cumulative normalised contribution to the flux measurements curve (CNF) was estimated as a function of distance from the measurement point. This curve was differentiated to obtain the relative contribution to the measured flux as a function of distance and was calculated for an average of all half-hour high wind speed ($\geq 8 \, m/s$) and low wind speed ($<8 \, m/s$) data normalised to a height of 10 m (U_{10} wind speed) for an oceanic fetch. These two curves are shown in Figure 4, with distance given on a logarithmic scale on the x-axis. The peak contribution, or most likely source region for both wind speed regimes was close to 1 km, verifying that the footprint was large enough for the majority of the fetch of interest to fall within it and thereby matching one of the key EC theory assumptions. The higher wind speed curve gives greater accuracy and confidence in locating the source region due to its narrower width and higher peak. The two black vertical lines represent upper and lower tidal limits (80 m and 180 m, resp.). The peak contribution for both high and low wind speeds was thus from significantly beyond the lower tidal limit, suggesting the impact of the tidal zone to be minimal and the measurement height of 22 m to be adequate.

Figure 5 shows a scatter plot of O_3 fluxes versus the corresponding O_3 mixing ratios. The latter varied between about 25 ppbv and 45 ppbv during the entire measurement period, that is, over a relatively small range. This may partially explain why a consistent relationship between both data sets was not evident. However, a moderately strong relationship between wind speed and O_3 fluxes was found as shown in
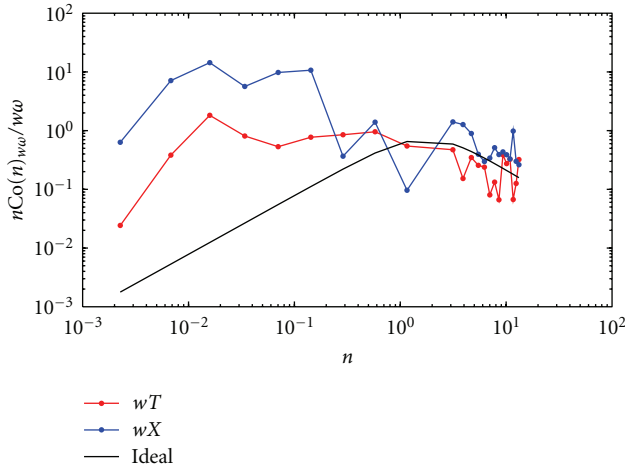
Figure 2: Averaged smoothed and normalized temperature cospectra (wT, in red) and O_3 cospectra (wX, in blue) for all O_3 flux values between $|0.01|$ and $|0.02| \, \mu g \, m^{-2} \, s^{-1}$. The symbols T, X, w, n, and ω represent temperature, O_3 signal, vertical wind speed component, and frequency, respectively. The theoretical (ideal) slope according to Kaimal et al. [27] displaying a $-4/3$ power law is also shown.
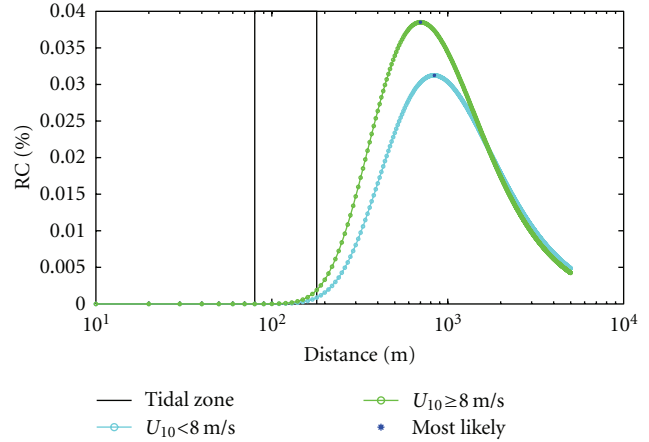
Figure 4: Relative flux contribution for EC measurements at 22 m height on the Mace Head tower. Footprint distance from the measurement location is shown on the x-axis. The tidal zone is represented by the two vertical black lines.
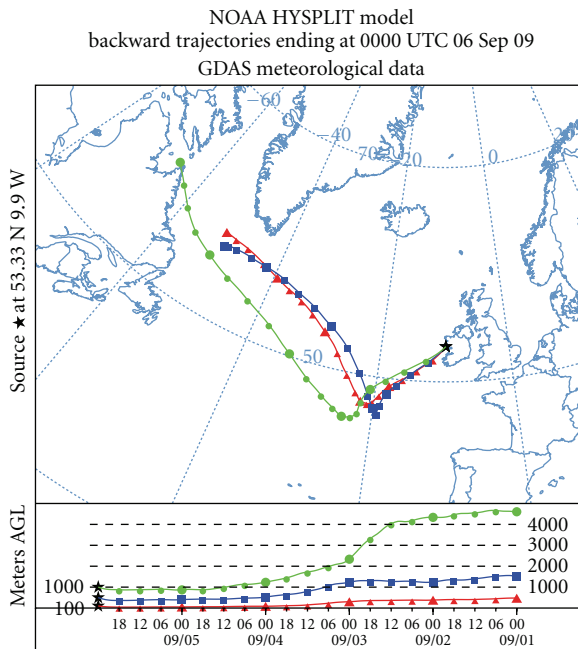
Figure 3: NOAA HYSPLIT back trajectories for Mace Head shown for period (2). These clean air sector trajectories were typical for all four periods shown in Figure 1. The red line shows 100 m, the blue line 500 m, and the green line 1000 m trajectory altitudes.

Figure 5: Scatter plot of O_3 fluxes versus O_3 mixing ratios showing a relatively low correlation between both data sets ($r^2 = 0.038$). High-tide and low-tide fluxes are also shown by different coloured symbols.

However, to a certain extent the scatter in the ozone flux data may also be due to chemical reactions in the atmospheric boundary and the sea surface layer. On the other hand, based on Aqua satellite observations by the MODIS (Moderate Resolution Imaging Spectroradiometer) instrument (http://oceancolor.gsfc.nasa.gov/products/chlo.html) we found no evidence for major phytoplankton blooms occurring in the footprint area during any of the observation periods. This may rule out the presence of high concentrations of reactive hydrocarbons affecting ozone deposition. With respect to the very low fluxes measured during the third period (also in the beginning of the fourth period) the red symbols in Figure 6 highlight the corresponding data showing that their magnitudes were independent of wind speed, and therefore other reasons must exist for their relatively small values.

O_3 fluxes were found to be both negative and positive in their direction of transport, which was not expected because

Figure 6. A power-law regression was applied and resulted in a best fit curve shown by the solid black line of the form $F_{O_3} = 7.75 \times 10^{-4} (U_{10})^{1.56}$. Ozone deposition fluxes tended to increase with higher wind speeds, which were coincident with the largest negative fluxes shown in Figure 1. Previously, McVeigh [20] reported a qualitatively similar relationship between wind speed and CO_2 fluxes measured at Mace Head.
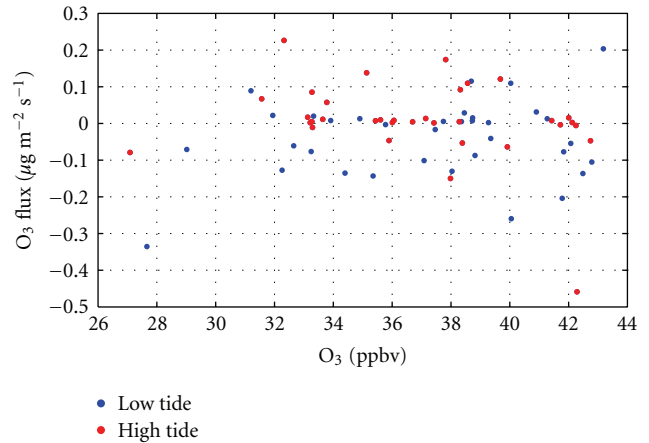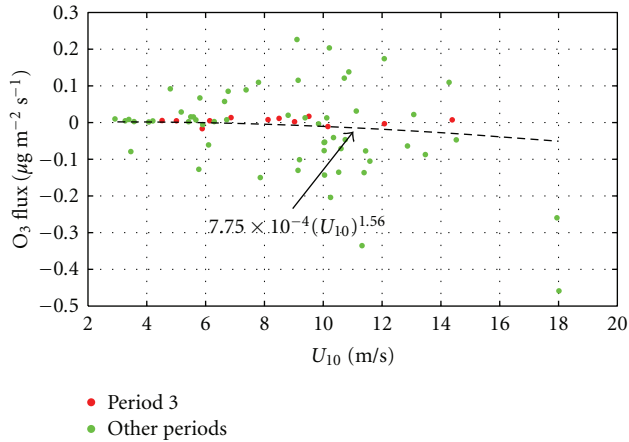
FIGURE 6: Relationship between 10 m wind speed and O_3 fluxes measured at 22 m. The black line represents the power-law relation between the 10 m wind speed and O_3 fluxes which was calculated as $F_{O_3} = 7.75 \times 10^{-4}(U_{10})^{1.56}$ ($r^2 = 0.344$). The red data points represent data from period (3) in Figure 1.

there are no processes at the sea surface that are known to produce O_3. A possible explanation for the positive fluxes may be signal noise since more flux values were measured below $-0.1\,\mu g\,m^{-2}\,s^{-1}$ than above $0.1\,\mu g\,m^{-2}\,s^{-1}$. However, given that the O_3 cospectra in Figure 2, which represent all fluxes between $|0.01|$ and $|0.02|\,\mu g\,m^{-2}\,s^{-1}$ exhibited a good shape and were similar to the temperature cospectra, noise was unlikely to be a major problem in this range.

6. Conclusions

First measurements of ozone fluxes during late summer and fall season have been conducted over shallow coastal waters west of Ireland based on the eddy flux covariance method. The results were comparable with previous studies at other coastal locations and over open ocean areas. We consider our results as baseline O_3 fluxes in the absence of major phytoplankton blooms which did not occur during the measurement periods in the footprint region as verified from satellite observations by the Aqua/MODIS instrument. The measurement height of 22 m was appropriate for excluding any significant influence by tidal movements on the measured fluxes. A diurnal signal was suggested by the average results but could not be statistically distinguished.

The main physical influence on O_3 fluxes was wind speed. Chemical reactions in the air and sea surface may have significantly influenced deposition rates, being the most plausible reason for the large degree of scatter observed. Although not highly significant, the power-law fit in Figure 6 points in a negative (downward) direction, consistent with the mean O_3 flux value measured in this study. Negative fluxes were expected according to theory, but the present results suggest that at the relatively small exchange rates encountered over open waters (compared to continental and exposed tidal environments) transport can occur in both directions, most likely due to its turbulent nature (see also [10]).

The current measurements are planned to be continued over a longer time period in order to investigate the seasonality of the fluxes, as well as any biological influences in more detail. Larger deposition rates are expected over regions with emissions from phytoplankton blooms due to increased chemical removal of ozone by reactions with hydrocarbons such as isoprene. Shipborne investigations during the occurrence of such blooms would be important to further establish the potential importance of the oceanic biosphere in curtailing atmospheric ozone levels with implications for particle nucleation, and to provide more data for corresponding global model simulations.
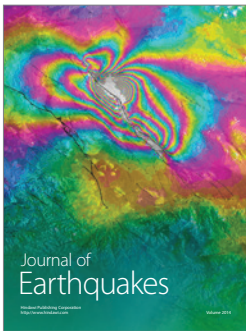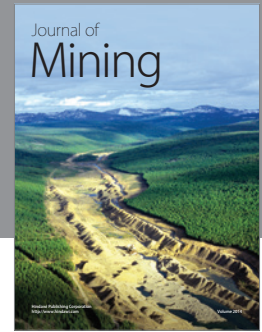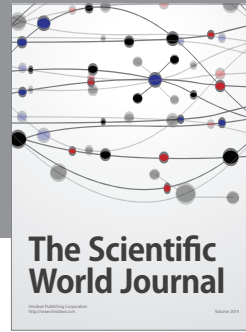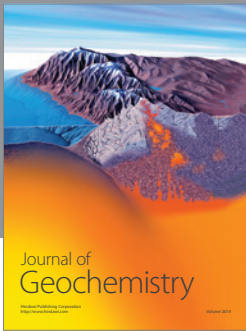
References

[1] R. G. Derwent, P. G. Simmonds, A. J. Manning, and T. G. Spain, "Trends over a 20-year period from 1987 to 2007 in surface ozone at the atmospheric research station, Mace Head, Ireland," *Atmospheric Environment*, vol. 41, no. 39, pp. 9091–9098, 2007.

[2] L. Ganzeveld, D. Helmig, C. W. Fairall, J. Hare, and A. Pozzer, "Atmosphere-ocean ozone exchange: a global modeling study of biogeochemical, atmospheric, and waterside turbulence dependencies," *Global Biogeochemical Cycles*, vol. 23, no. 4, 16 pages, 2009.

[3] D. I. Reeser, A. Jammoul, D. Clifford et al., "Photoenhanced reaction of ozone with chlorophyll at the seawater surface," *Journal of Physical Chemistry C*, vol. 113, no. 6, pp. 2071–2077, 2009.

[4] D. Clifford, D. J. Donaldson, M. Brigante, B. D'Anna, and C. George, "Reactive uptake of ozone by chlorophyll at aqueous surfaces," *Environmental Science and Technology*, vol. 42, no. 4, pp. 1138–1143, 2008.

[5] M. Martino, G. P. Mills, J. Woeltjen, and P. S. Liss, "A new source of volatile organoiodine compounds in surface seawater," *Geophysical Research Letters*, vol. 36, no. 1, Article ID L01609, 2009.

[6] W. Chang, B. G. Heikes, and M. Lee, "Ozone deposition to the sea surface: chemical enhancement and wind speed dependence," *Atmospheric Environment*, vol. 38, no. 7, pp. 1053–1059, 2004.

[7] G. McFiggans, H. Coe, R. Burgess et al., "Direct evidence for coastal iodine particles from Laminaria macroalgae—linkage to emissions of molecular iodine," *Atmospheric Chemistry and Physics*, vol. 4, no. 3, pp. 701–713, 2004.

[8] C. D. O'Dowd, J. L. Jimenez, R. Bahreini et al., "Marine aerosol formation from biogenic iodine emissions," *Nature*, vol. 417, no. 6889, pp. 632–636, 2002.

[9] J. D. Whitehead, G. B. Mcfiggans, M. W. Gallagher, and M. J. Flynn, "Direct linkage between tidally driven coastal ozone deposition fluxes, particle emission fluxes, and subsequent CCN formation," *Geophysical Research Letters*, vol. 36, no. 4, 5 pages, 2009.

[10] L. Bariteau, D. Helmig, C. W. Fairall, J. E. Hare, J. Hueber, and E. K. Lang, "Determination of oceanic ozone deposition by ship-borne eddy covariance flux measurements," *Atmospheric Measurement Techniques*, vol. 2, no. 4, pp. 1933–1972, 2009.

[11] M. W. Gallagher, K. M. Beswick, and H. Coe, "Ozone deposition to coastal waters," *Quarterly Journal of the Royal Meteorological Society*, vol. 127, no. 572, pp. 539–558, 2001.

[12] M. W. Gallagher, K. M. Beswick, G. McFiggans, H. Coe, and T. W. Choularton, "Ozone dry deposition velocities for coastal waters," *Water, Soil, and Air Pollution: Focus*, vol. 1, no. 5-6, pp. 233–242, 2001.

[13] L. Coleman, S. Varghese, O. P. Tripathi, S. G. Jennings, and C. D. O'Dowd, "Investigating the chemical impact of iodide on ozone deposition to the ocean in the North Atlantic using regional climate model REMOTE," *Advances in Meteorology*.

[14] S. G. Jennings, C. Kleefeld, C. D. O'Dowd et al., "Mace Head Atmospheric Research Station—characterization of aerosol radiative parameters," *Boreal Environment Research*, vol. 8, no. 4, pp. 303–314, 2003.

[15] T. C. O'Connor, S. G. Jennings, and C. D. O'Dowd, "Highlights of fifty years of atmospheric aerosol research at Mace Head," *Atmospheric Research*, vol. 90, no. 2–4, pp. 338–355, 2008.

[16] M. Coyle, *The gaseous exchange of ozone at terrestrial surfaces: non-stomatal deposition to grassland*, Ph.D. thesis, University of Edinburgh, 2005.

[17] H. Gusten, G. Heinrich, R. W. H. Schmidt, and U. Schurath, "A novel ozone sensor for direct eddy flux measurements," *Journal of Atmospheric Chemistry*, vol. 14, no. 1–4, pp. 73–84, 1992.

[18] E. G. Norton, G. Vaughan, J. Methven et al., "Boundary layer structure and decoupling from synoptic scale flow during NAMBLEX," *Atmospheric Chemistry and Physics*, vol. 6, no. 2, pp. 433–445, 2006.

[19] G. J. Kunz and G. De Leeuw, "Micrometeorological characterisation of the Mace Head field station during PARFORCE," in *New Particle Formation and Fate in the Coastal Environment (PARFORCE)*, C. O'Dowd and K. Hämeri, Eds., vol. 48 of *Rep. Ser. Aerosol Sci.*, pp. 5–62, Finn. Assoc. Aerosol Res., Helsinki, Finland, 2000.

[20] P. McVeigh, *Micrometeorological and CO2 fluxes in the coastal environment*, Ph.D. thesis, School of Physics, National University of Ireland Galway, 2009.

[21] D. Ceburnis, C. D. O'Dowd, G. S. Jennings et al., "Marine aerosol chemistry gradients: elucidating primary and secondary processes and fluxes," *Geophysical Research Letters*, vol. 35, no. 7, Article ID L07804, 2008.

[22] M. Geever, C. D. O'Dowd, S. van Ekeren et al., "Submicron sea spray fluxes," *Geophysical Research Letters*, vol. 32, no. 15, Article ID L15810, 2005.

[23] G. Buzorius, U. Rannik, J. M. Mäkelä, T. Vesala, and M. Kulmala, "Vertical aerosol particle fluxes measured by eddy covariance technique using condensational particle counter," *Journal of Aerosol Science*, vol. 29, no. 1-2, pp. 157–171, 1998.

[24] J. H. Duyzer, G. Deinum, and J. Baak, "The interpretation of measurements of surface exchange of nitrogen oxides, corrections for chemical reactions," *Philosophical Transactions of the Royal Society A*, vol. 351, pp. 231–248, 1995.

[25] J. B. A. Muller, C. J. Percival, M. W. Gallagher, D. Fowler, M. Coyle, and E. Nemitz, "Sources of uncertainty in eddy covariance ozone flux measurements made by dry chemiluminescence fast response analysers," *Atmospheric Measurement Techniques*, vol. 3, no. 1, pp. 163–176, 2010.

[26] E. K. Webb, G. I. Pearman, and R. Leuning, "Correction of flux measurements for density effects due to heat and water vapour transfer," *Quarterly Journal Royal Meteorological Society*, vol. 106, no. 447, pp. 85–100, 1980.

[27] J. C. Kaimal, Y. Izumi, J. C. Wyngaard, and R. Cote, "Spectral characteristics of surface-layer turbulence," *Quarterly Journal of the Royal Meteorological Society*, vol. 98, no. 417, pp. 563–589, 1972.

[28] P. H. Schuepp, M. Y. Leclerc, J. I. MacPherson, and R. L. Desjardins, "Footprint prediction of scalar fluxes from analytical solutions of the diffusion equation," *Boundary-Layer Meteorology*, vol. 50, no. 1–4, pp. 355–373, 1990.